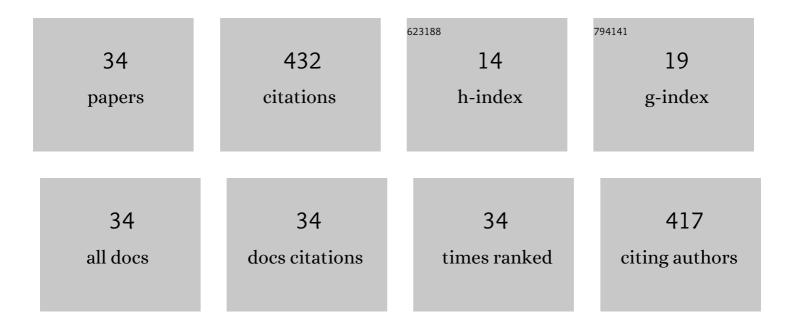
De-Sheng Liu

List of Publications by Year in descending order

Source: https://exaly.com/author-pdf/6386325/publications.pdf Version: 2024-02-01



#	Article	IF	CITATIONS
1	A bifunctional GeC/SnSSe heterostructure for highly efficient photocatalysts and photovoltaic devices. Nanoscale, 2022, 14, 7292-7302.	2.8	24
2	High mobility and enhanced photoelectric performance of two-dimensional ternary compounds NaCuX (X = S, Se, and Te). Physical Chemistry Chemical Physics, 2021, 23, 2475-2482.	1.3	22
3	Design of a noble-metal-free direct Z-scheme photocatalyst for overall water splitting based on a SnC/SnSSe van der Waals heterostructure. Physical Chemistry Chemical Physics, 2021, 23, 21641-21651.	1.3	30
4	Giant and robust intrinsic spin Hall effects in metal dihydrides: A first-principles prediction. Physical Review B, 2021, 103, .	1.1	6
5	Prediction of crossing nodal-lines and large intrinsic spin Hall conductivity in topological Dirac semimetal Ta3As family. Npj Computational Materials, 2021, 7, .	3.5	14
6	Robust Topological Nodal-Line Semimetals from Periodic Vacancies in Two-Dimensional Materials. Journal of Physical Chemistry Letters, 2021, 12, 5710-5715.	2.1	6
7	First principles study of photoelectrochemical water splitting in monolayer Sn2S2P4 with high solar-to-hydrogen efficiency. Applied Physics Letters, 2021, 119, .	1.5	17
8	Rational design of magnetic semiconductors of longitudinal silicene/III-V compound heteronanoribbons. Applied Surface Science, 2020, 501, 144230.	3.1	1
9	Rational design of [<i>e</i>]-fusion induced high-performance DHP/CPD based photoswitches. Physical Chemistry Chemical Physics, 2020, 22, 26255-26264.	1.3	2
10	Spin-polarized current in wide bandgap hexagonal boron nitrides containing 4 8 line defects. Computational Materials Science, 2020, 183, 109799.	1.4	4
11	Large room-temperature valley polarization by valley-selective switching of exciton ground state. Physical Review B, 2020, 101, .	1.1	18
12	Theoretical Simulations of Heavy-Atom Kinetic Isotope Effects in Aliphatic Claisen Rearrangement. Journal of Physical Chemistry A, 2020, 124, 10678-10686.	1.1	1
13	Exotic magnetism in As-doped α/β-In ₂ Se ₃ monolayers with tunable anisotropic carrier mobility. Physical Chemistry Chemical Physics, 2019, 21, 19234-19241.	1.3	18
14	Rational Design of Reversible Molecular Photoswitches Based on Diarylethene Molecules. Journal of Physical Chemistry C, 2019, 123, 2736-2745.	1.5	8
15	Dynamical Simulations of Polaron Spin-Filtering and Rectification in an Organic Magnetic–Nonmagnetic Co-oligomer: The Interfacial Effect. Journal of Physical Chemistry C, 2019, 123, 14432-14438.	1.5	4
16	Spin transport properties in Fe-doped graphene/hexagonal boron-nitride nanoribbons heterostructures. Physics Letters, Section A: General, Atomic and Solid State Physics, 2019, 383, 2217-2222.	0.9	3
17	Enhanced photocatalysis for water splitting in layered tin chalcogenides with high carrier mobility. Physical Chemistry Chemical Physics, 2019, 21, 7559-7566.	1.3	36
18	Lateral scaling and positioning effects of top-gate electrodes on single-molecule field-effect transistors. Journal of Physics Condensed Matter, 2019, 31, 285302	0.7	2

DE-SHENG LIU

#	Article	IF	CITATIONS
19	Impact of interface types on spin transport in heterostructures of graphene/hexagonal boron-nitride nanoribbons. Organic Electronics, 2018, 58, 63-68.	1.4	6
20	Adsorption of gas molecules on a manganese phthalocyanine molecular device and its possibility as a gas sensor. Physical Chemistry Chemical Physics, 2018, 20, 2048-2056.	1.3	40
21	Chemically Functionalized Penta-stanene Monolayers for Light Harvesting with High Carrier Mobility. Journal of Physical Chemistry C, 2018, 122, 21763-21769.	1.5	18
22	Tuning spin-filtering, rectifying, and negative differential resistance by hydrogenation on topological edge defects of zigzag silicene nanoribbons. Physics Letters, Section A: General, Atomic and Solid State Physics, 2018, 382, 2475-2483.	0.9	7
23	Edge hydrogenation-induced spin-filtering and negative differential resistance effects in zigzag silicene nanoribbons with line defects. RSC Advances, 2017, 7, 25244-25252.	1.7	17
24	Creation of half-metallic <mml:math xmlns:mml="http://www.w3.org/1998/Math/MathML"><mml:mi>f</mml:mi> -orbital Dirac fermion with superlight elements in orbital-designed molecular lattice. Physical Review B, 2017, 96, .</mml:math 	1.1	10
25	The electronic transport properties of zigzag silicene nanoribbon slices with edge hydrogenation and oxidation. Physical Chemistry Chemical Physics, 2016, 18, 11513-11519.	1.3	26
26	Role of edge dehydrogenation in magnetization and spin transport of zigzag graphene nanoribbons with line defects. Organic Electronics, 2015, 27, 212-220.	1.4	5
27	Electronic Transport of a Molecular Photoswitch with Graphene Nanoribbon Electrodes. Chinese Physics Letters, 2014, 31, 057304.	1.3	4
28	Electronic transport properties of a dithienylethene-based polymer with different metallic contacts. RSC Advances, 2014, 4, 40941-40950.	1.7	6
29	Effect of the orientation of nitro group on the electronic transport properties in single molecular field-effect transistors. Physical Chemistry Chemical Physics, 2013, 15, 832-836.	1.3	6
30	A possible salicylideneanilines-based optical molecular switch induced by a reversible hydrogen transfer: an <i>ab initio</i> study. Molecular Physics, 2011, 109, 209-215.	0.8	7
31	EFFECT OF TORSION ANGLE IN 4,4′-BIPHENYLDITHIOL FUNCTIONALIZED MOLECULAR JUNCTION. International Journal of Modern Physics B, 2011, 25, 699-710.	1.0	1
32	Intrachain polaron motion and geminate combination in donor-acceptor copolymers: Effects of level offset and interfacial coupling. Physical Review B, 2008, 78, .	1.1	25
33	Bloch oscillations in a one-dimensional organic lattice. Physical Review B, 2006, 74, .	1.1	30
34	Effect of atomic disorder or chain length on the stability of photoinduced polarization inversion. Journal of Chemical Physics, 2002, 116, 6760-6763.	1.2	8